Electronic Supplementary Information

Experimental

Materials: Hydrochloric acid (HCl), nitric acid (HNO_3), and ethanol (C_2H_5OH) were purchased from Chengdu Kelong Chemical Reagent Factory. Nafion (5 wt%) was obtained from Sigma-Aldrich Chemical Reagent Co., Ltd. ammonium chloride (NH_4Cl), hydrazine monohydrate ($N_2H_4\cdot H_2O$), sodium hypochlorite (NaClO), and carbon paper were bought from Beijing Chemical Corporation. Bismuth (III) nitrate pentahydrate ($Bi(NO_3)_3\cdot 5H_2O$), sodium citrate ($Na_3C_6H_5O_7\cdot 2H_2O$), salicylic acid ($C_7H_6O_3$), sodium nitroferricyanide dihydrate ($C_5FeN_6Na_2O\cdot 2H_2O$), and para-(dimethylamino) benzaldehyde (p-$C_9H_{11}NO$) were purchased from Aladdin Ltd, Shanghai, China. High-purity N_2 (99.999%) and Ar (99.999%) were purchased from Chengdu Xuyuan Chemical Co., Ltd., China. All the chemicals were analytical grade and used without further purification. Ultra-pure water from a Milli-Q water purification system was used throughout all experiments.

Preparation of Bi nanodendrite (Bi ND): Bi ND was synthesized via electrodeposition on Ti film. The Ti film was rinsed thoroughly through acetone, ethanol, and deionized water. The potentiostatic electrodeposition was conducted in a standard three electrode system, which the working electrode, reference electrode and counter electrode were Ti film, Ag/AgCl/saturated KCl solution, and platinum plate, respectively. The plating solution was consisted of 1.0 M HNO_3 and 1 mM $Bi(NO_3)_3$, which was deaerated with Ar before every experiment. The electrodeposition was performed according to two-step procedures (1) at −0.5V for 200 s；(2) at −0.8 V for 1000 s. Then the prepared sample was rinsed thoroughly with deionized water until the peak of nitrate could not be measured by UV-Vis absorption spectra. We then choosed to scrape down the electrocatalyst from the Ti film and prepared homogeneous ink.

Preparation of Bi nanosphere (Bi NS): 0.973g $Bi(NO_3)_3\cdot 5H_2O$ was dissolved into 20 mL of ethylene glycol (EG) with constant stirring. Then the mixed solution was transferred into 30 mL Teflon-lined autoclave and maintained at 220 ^oC for 6 h.

Finally, the obtained products were centrifuged and washed thoroughly with deionized water and dried in an air oven at 80 ^oC overnight.

Preparation of Bi ND/CP and Bi NS/CP: First, CP was cleaned via sonication with ethanol and water for several times and dried in the oven. Then, 5 mg of Bi ND or Bi NS and 20 μL of Nafion solution (5 wt%) was dispersed in 980 μL ethanol follow by 30 min sonication to form a homogeneous ink. Finally, 20 μL ink was loaded on a piece of CP (1×1 cm^{-2}) and dried under ambient condition.

Characterizations: XRD patterns were obtained from a Shimazu XRD-6100 diffractometer with Cu Kα radiation (40 kV, 30 mA) of wavelength 0.154 nm (Japan). Scanning electron microscopy (SEM) images were collected on a GeminiSEM 300 scanning electron microscope (ZEISS, Germany) at an accelerating voltage of 5 kV. Transmission electron microscopy (TEM) images were obtained on a HITACHI H-8100 electron microscopy (Hitachi, Tokyo, Japan) operated at 200 kV. The ion chromatography data were conducted and collected on Metrohm 940 Professional IC Vario. The absorbance data of spectrophotometer were measured on UV-2700 ultraviolet-visible (UV-Vis) spectrophotometer.

Electrochemical measurement: The electrochemical NRR performance measurement were carried out in a two-compartment cell separated by Nafion 117 membrane using a CHI 660E electrochemical analyzer (CHI Instruments, Inc., Shanghai). Before electrochemical measurement, the Nafion membrane was first boiling in ultrapure water for 1 h and soaked in H_2O_2 (5 wt%) at 80 ˚C for another 1 h then the membrane was treated in 0.5 M H_2SO_4 for 3 h at 80 ˚C and finally rinsed with deionized water. The electrochemical experiments were performed on a three-electrode system, which the graphite rod as the counter electrode, Ag/AgCl/saturated KCl solution as the reference electrode and the Bi ND/CP was used as working electrode. All experiments were performed at room temperature and pressure. Additionally, the 0.1 M HCl electrolyte was bubbled with high-purity N_2 (99.999%) for 30 min before NRR measurements. For N_2 electroreduction experiments, potentiostatic test was carried out in N_2-saturated 0.1 M HCl solution. The double layer capacitance is measured by cyclic voltammetry. A potential range from 0 to 0.10 vs. Ag/AgCl is chosen for the

CV test under different scan rates of 20, 40, 60, 80, 100, 120 mV s^{-1} without faradic current. The differences of positive and negative current density at the potential-range center were plotted vs. scan rates, the slope of curves were double capacitance. Notably, all potentials reported in this work were converted to reversible hydrogen electrode (RHE) scale via calibration with the following equation:

$$E\ (RHE) = E\ (Ag/AgCl) + 0.059 \times pH + E^{\theta}\ (Ag/AgCl)$$

Determination of NH_3: The indophenol blue method was used to quantify concentration of the produced NH_3 in electrolyte by ultraviolet-visible (UV-Vis) spectrophotometer.[1] In 0.1 M HCl, 2 mL HCl electrolyte was taken from the cathodic chamber, and then 2 mL of 1 M NaOH solution containing 5% salicylic acid and 5% sodium citrate was added into this solution. Subsequently, 1 mL of 0.05 M NaClO and 0.2 mL of 1% $C_5FeN_6Na_2O\cdot 2H_2O$ were add into the above solution. After standing at room temperature and keeping out of the light for 2 h, the UV-Vis absorption was measured at a wavelength of 655 nm. The concentration-absorbance curve was calibrated using standard NH_4^+ solution with NH_3 concentrations of 0.0, 0.05, 0.10, 0.15, 0.20, 0.25, and 0.30 μg mL^{-1} in 0.1 M HCl. The fitting curve ($y = 0.36x + 0.052$, $R^2 = 0.999$) shows good linear relation of absorbance value with NH_3 concentration by three times independent calibrations.

Determination of N_2H_4: N_2H_4 concentration in the HCl electrolyte was determined by the method of Watt and Chrisp.[2] Firstly, the mixture solution of 5.99 g p-$C_9H_{11}NO$, 30 mL HCl and 300 mL ethanol was used as a color reagent. Then 5 mL electrolyte was removed from the electrochemical reaction vessel, and added into 5 mL prepared color reagent and stirred 20 min at room temperature. the absorbance of such solution at the absorbance of 455 nm was measured to quantify the hydrazine yields, the fitting curve ($y = 0.76x + 0.048$, $R^2 = 0.9999$) shows good linear relation of absorbance value with N_2H_4 concentration by three times independent calibrations.

Calculations of NH_3 yield and Faradaic efficiency (FE): The Faradic efficiency (FE) for N_2 reduction was defined as the amount of electric charge used for synthesizing NH_3 divided the total charge passed through the electrodes during the electrolysis. The total amount of NH_3 produced was measured using colorimetric methods.

Assuming three electrons were needed to produce one NH_3 molecule, the FE could be calculated as follows:

$$FE = 3 \times F \times [NH_3] \times V / (17 \times Q) \times 100\%$$

The rate of NH_3 yield was calculated using the following equation:

$$NH_3 \text{ yield} = [NH_3] \times V / (m_{cat.} \times t)$$

The amount of NH_3 was calculated as follows:

$$m_{NH3} = [NH_3] \times V$$

Where F is the Faraday constant (96500 C mol^{-1}); $[NH_3]$ is the measured NH_3 concentration; V is the volume of the electrolyte in the cathodic chamber (35 mL); Q is the total quantity of applied electricity; $m_{cat.}$ is the loaded mass of catalyst on carbon paper (0.1 mg) and t is the reduction time (2 h).

Colorimetric detection of NO_3^-: The amount of NO_3^- in the supernatant of the washed sample can be quantitatively determined by spectrophotometer measurement.[3] Typically, 5 mL of standard $LiNO_3$ solution and added into 0.10 mL of 1.0 M HCl. After standing for 5 min, the various concentration of NO_3^- was measured using UV-Vis spectrophotometer at wavelength range from 200 nm to 300 nm. The fitting curve ($y = 0.087x + 0.0003$, $R^2 = 0.997$) shows good linear relation between the absorbance value and NO_3^- concentration by three times independent calibrations.

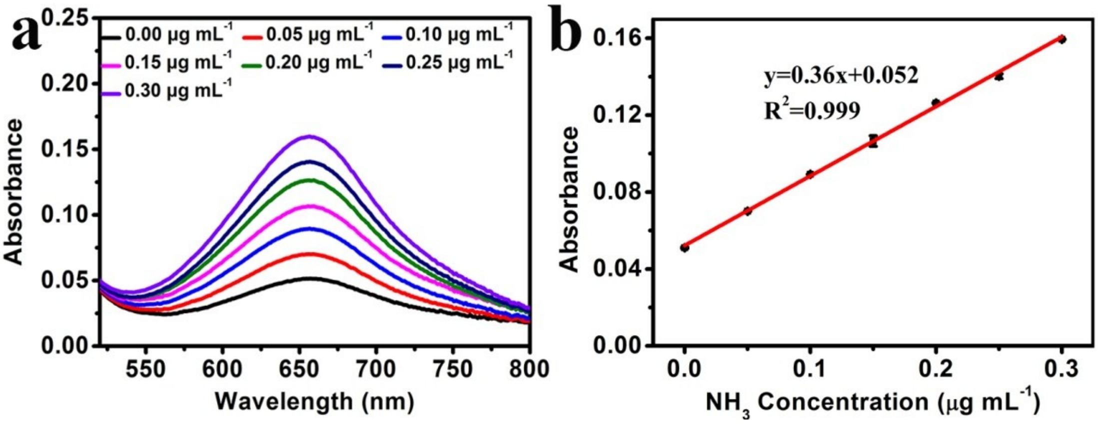

Fig. S1. (a) UV-Vis absorption curves of indophenol assays with NH_3 concentrations after incubated for 2 h at room temperature in 0.1 M HCl. (b) Calibration curve used for estimation of NH_3.

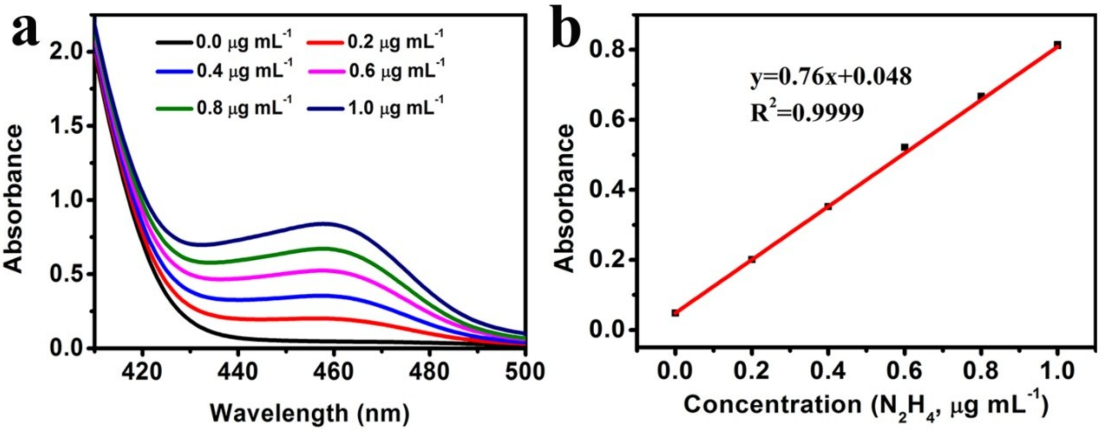

Fig. S2. (a) UV-Vis absorption spectra of N_2H_4 concentrations after incubated for 20 min at room temperature. (b) Calibration curve used for calculation of N_2H_4 concentrations.

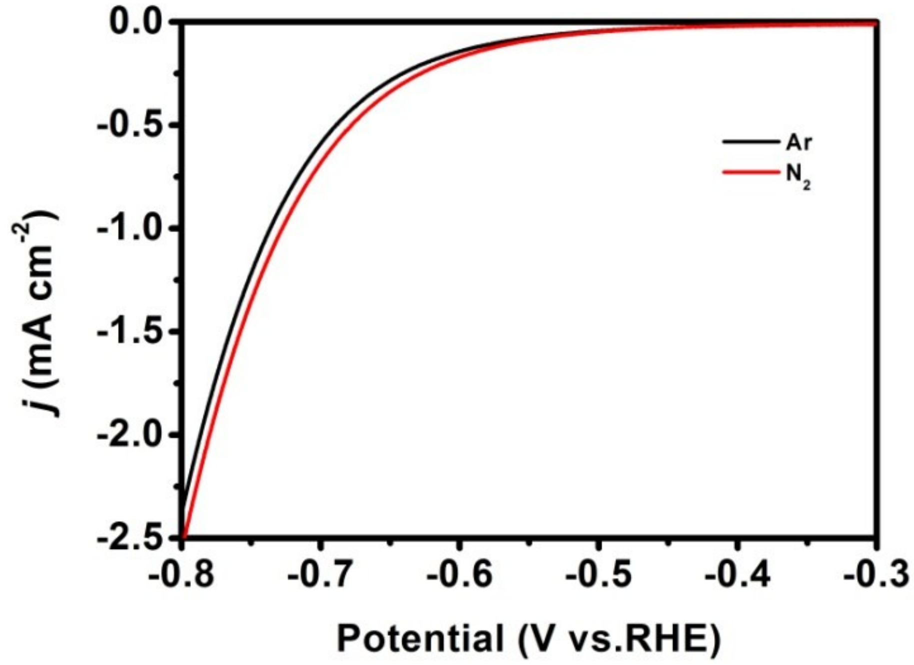

Fig. S3. LSV curves of Bi ND/CP in N_2-saturated and Ar-saturated 0.1 M HCl electrolyte at a scan rate of 5 mV s^{-1}.

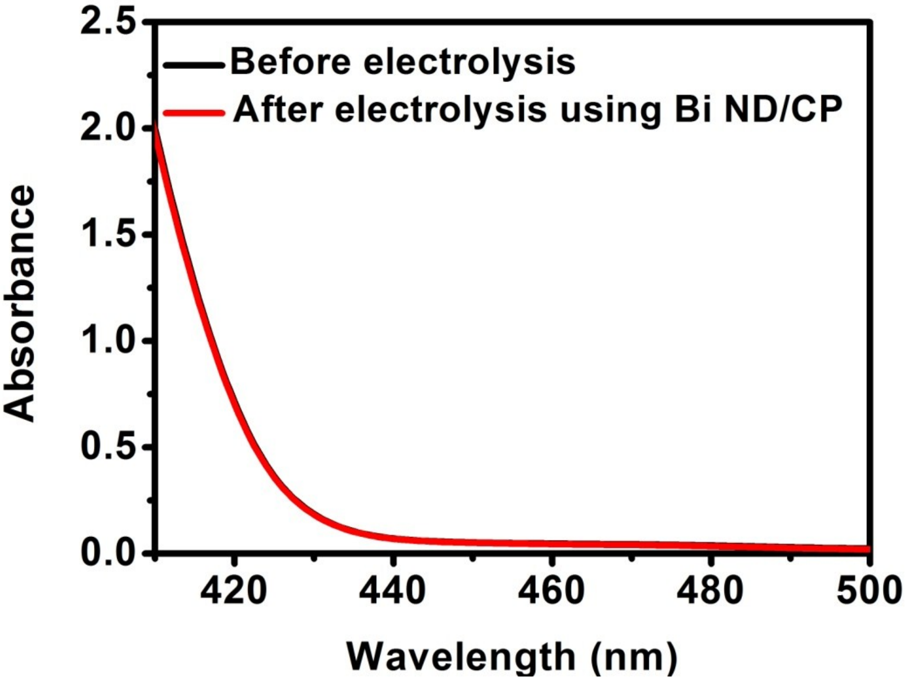

Fig. S4. UV-Vis absorption curves of the electrolytes treated with the method of Watt and Crisp for 20 min after NRR at a series of potentials.

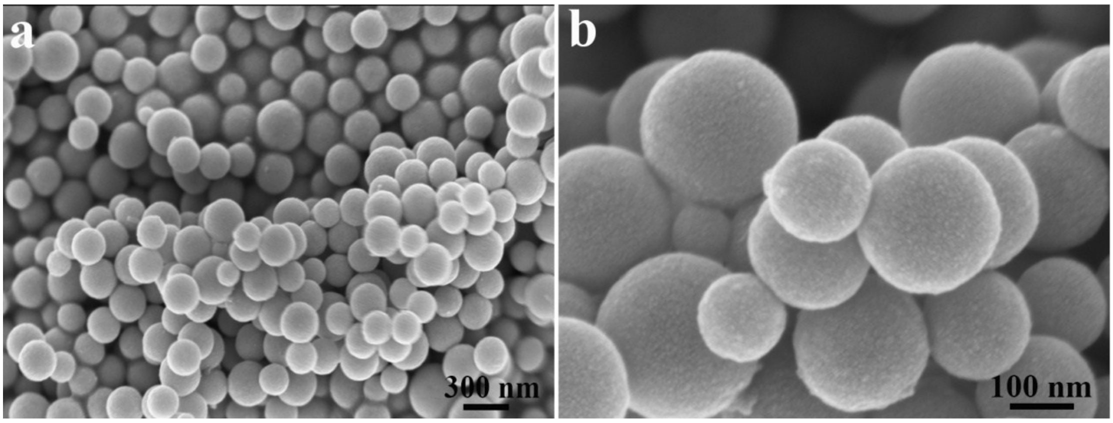

Fig. S5. SEM images of Bi nanospheres.

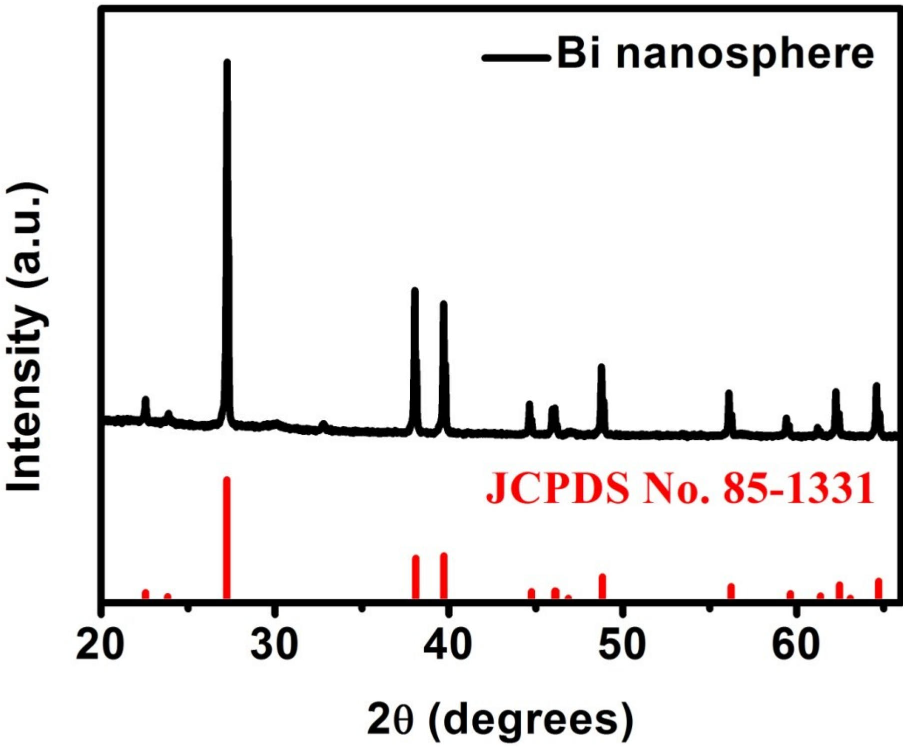

Fig. S6. XRD pattern of Bi nanospheres.

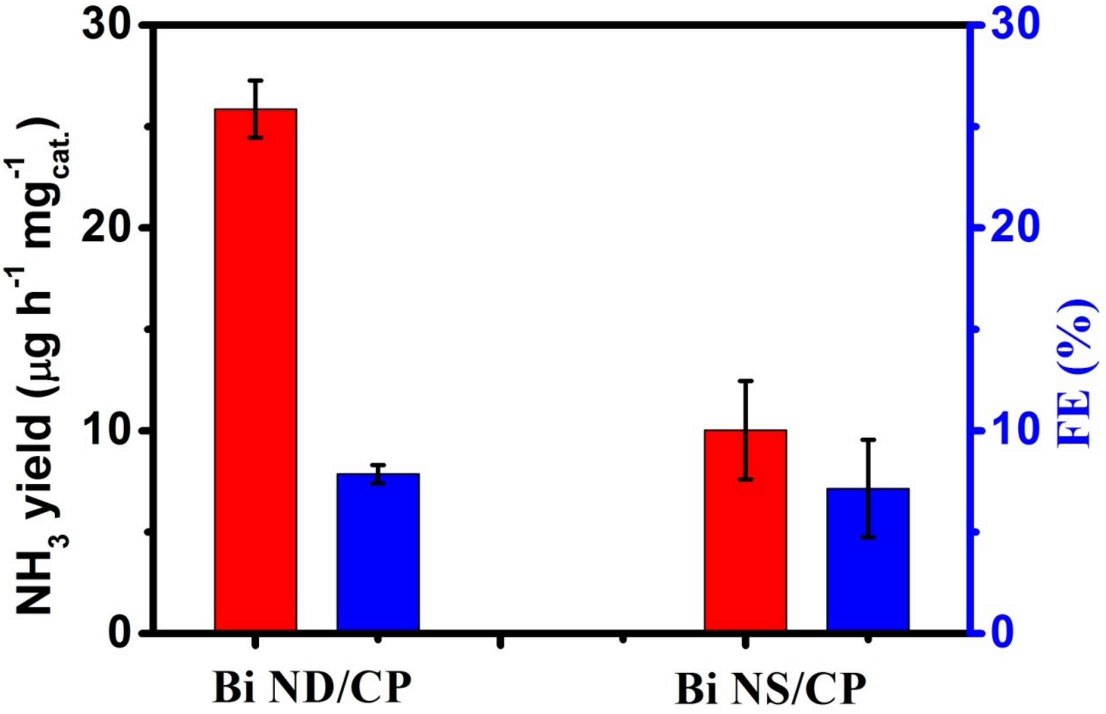

Fig. S7. NH_3 yield and FEs at -0.60 V for 2 h over Bi ND/CP and Bi NS/CP after testing 2 h for three times.

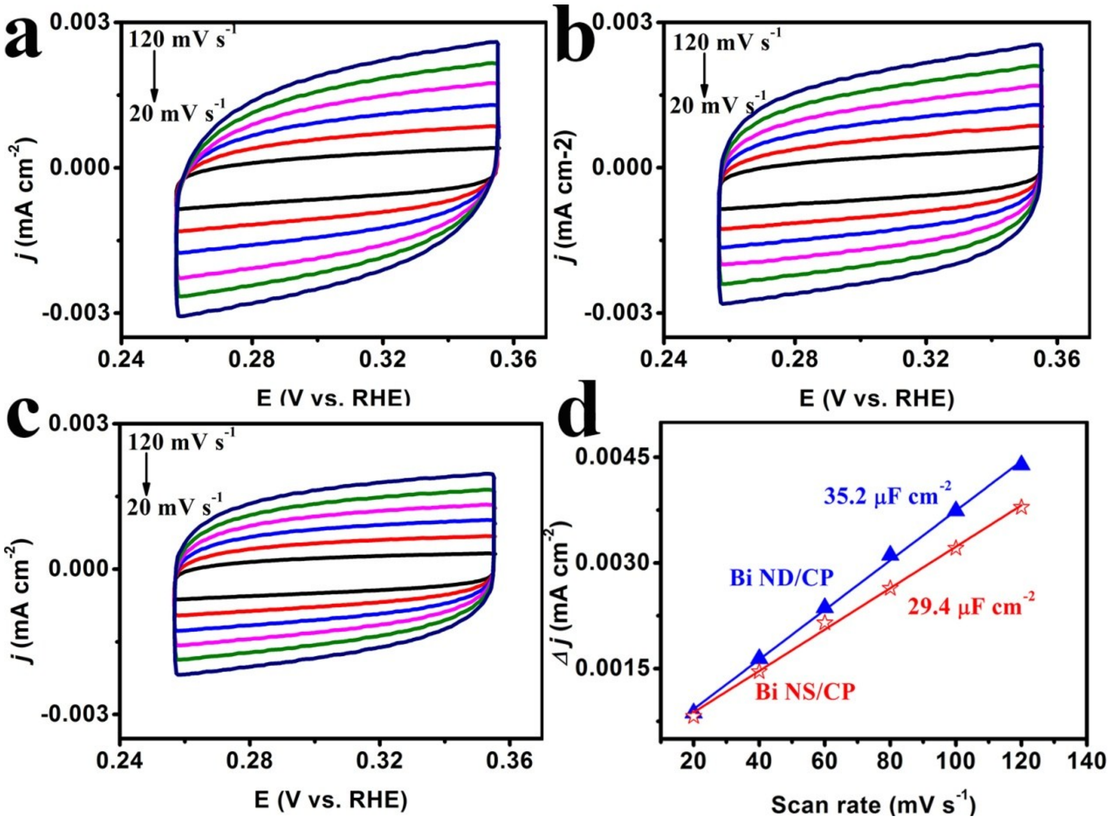

Fig. S8. CVs of (a) Bi ND/CP, (b) Bi NS/CP and (c) bare CP in the non-faradaic capacitance current range with various scan rates (20-120 mV s^{-1}) in the region of 0.256 to 0.356 V vs. RHE. (d) Corresponding capacitive currents at 0.306 V vs. RHE as a function of scan rates for Bi ND/CP and Bi NS/CP.

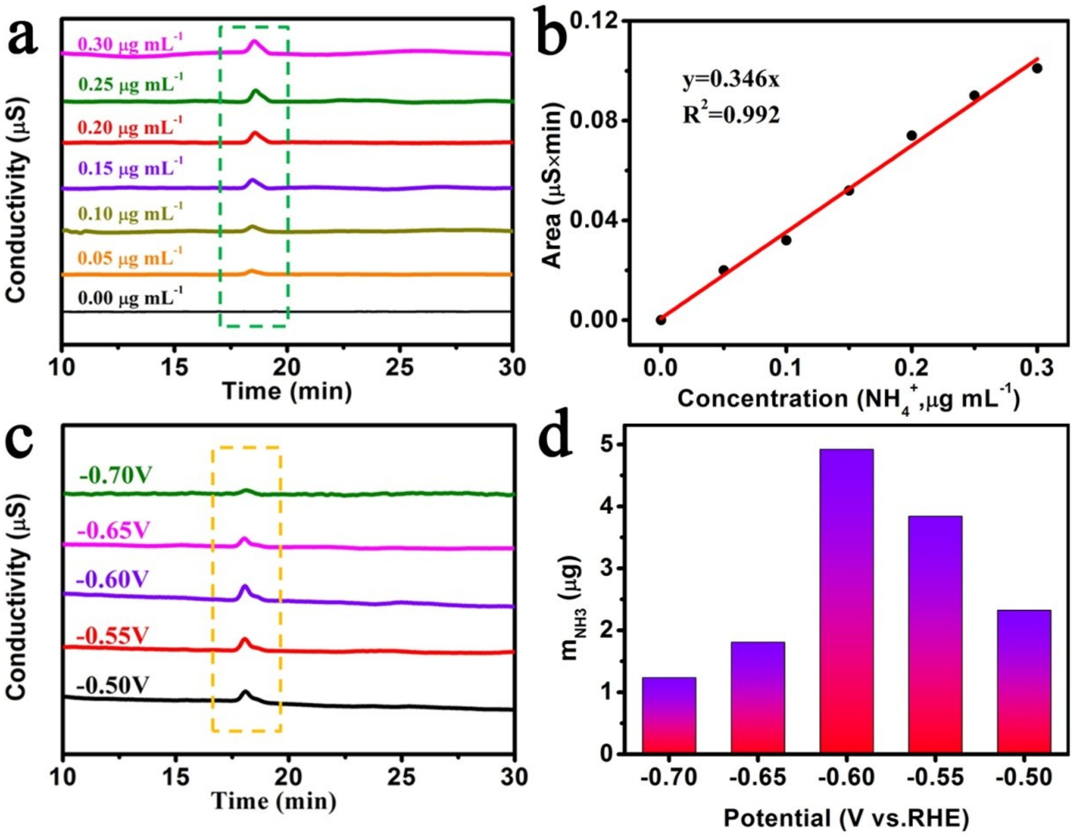

Fig. S9. (a) Ion chromatograms of NH_4Cl with various concentrations in 0.1 M HCl. (b) Calibration curve used for estimation of NH_3. (c) Curves of ion chromatography of Bi ND/CP after NRR electrolysis at different potentials for 2 h. (d) m_{NH3} of Bi ND/CP for the N_2 reduction at a series of potentials attained by ion chromatography.

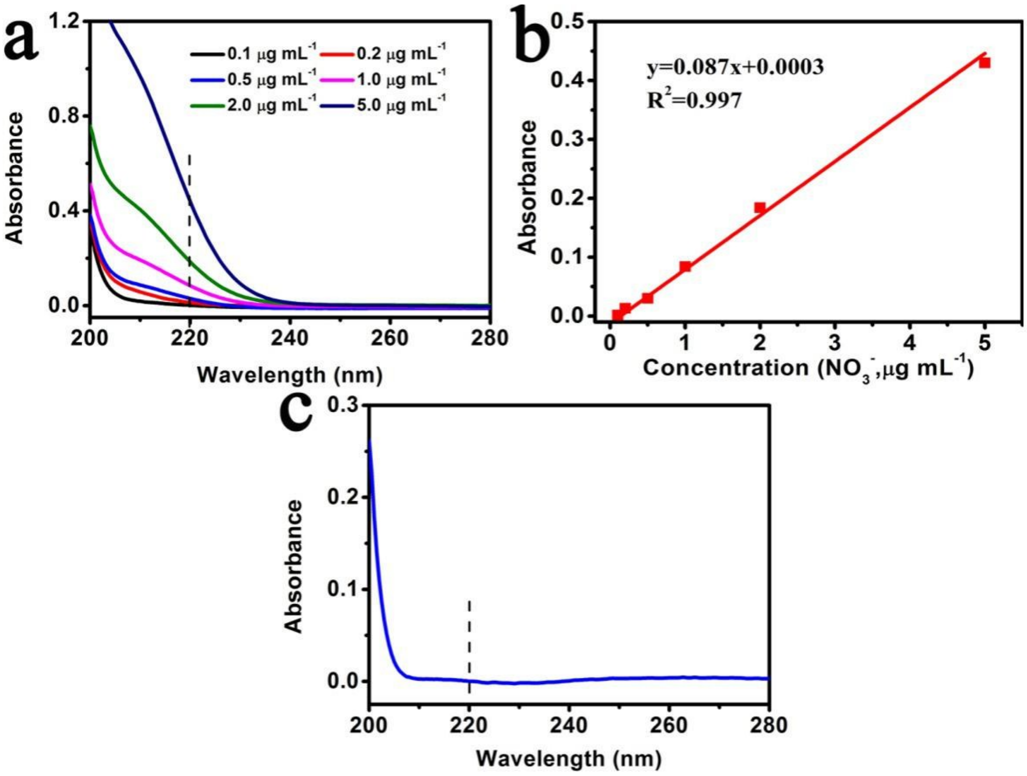

Fig. S10. (a) UV-Vis absorption spectra of different concentrations of $LiNO_3$. (b) Calibration curve used for calculating the concentration of NO_3^-. (c) UV-Vis absorption spectra for the determination of NO_3^- in the supernatant of the washed dendritic Bi.

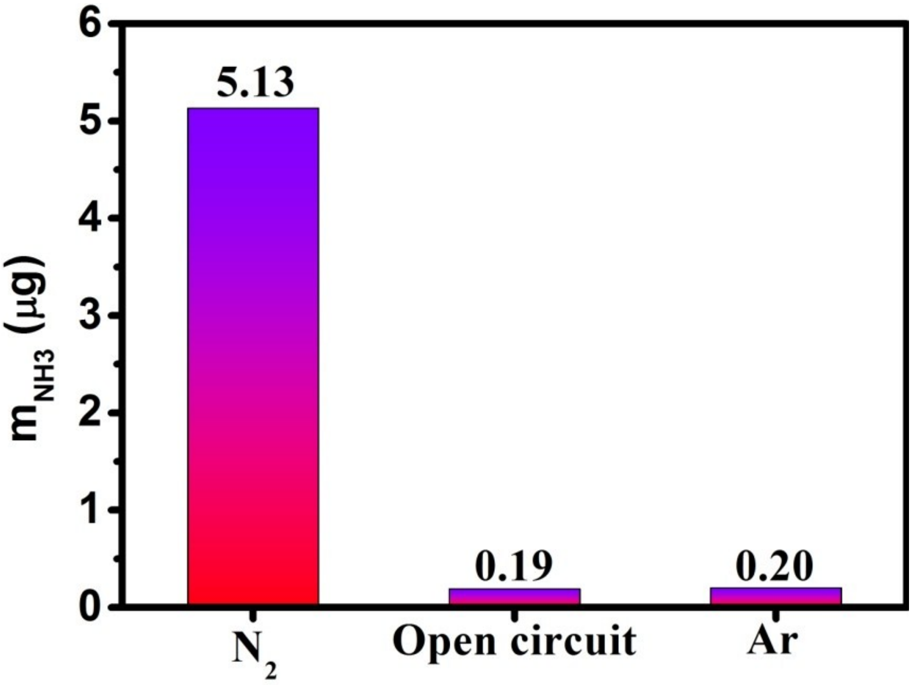

Fig. S11. Comparison of amount of NH_3 generated under different conditions.

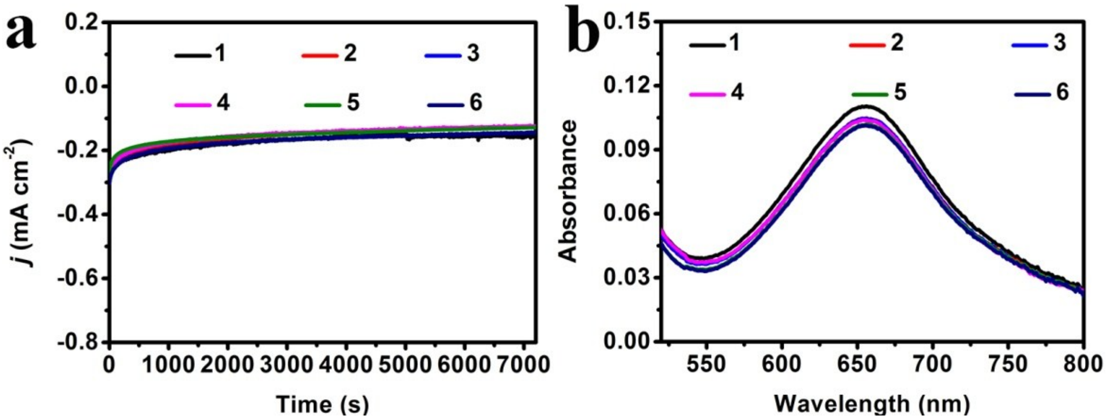

Fig. S12. (a) Time-dependent current density curves of Bi ND/CP electrode at –0.60 V over 6 cycles. (b) UV-Vis absorption spectra of the electrolytes stained with indophenol indicator after 2 h NRR electrolysis at –0.60 V over 6 cycles.

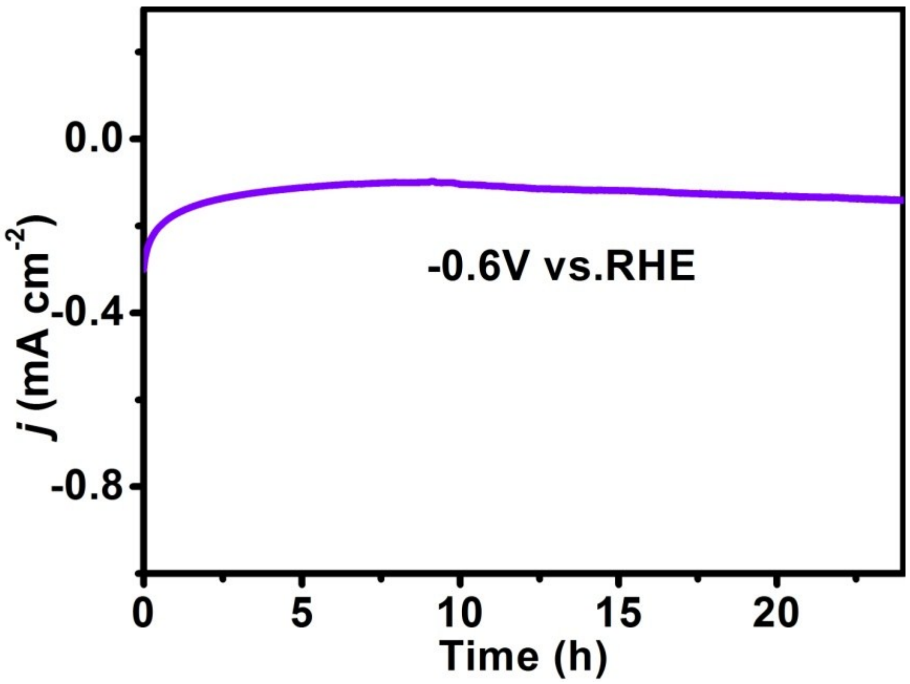

Fig. S13. Time-dependent current density curve for Bi ND/CP at –0.60 V for 24 h.

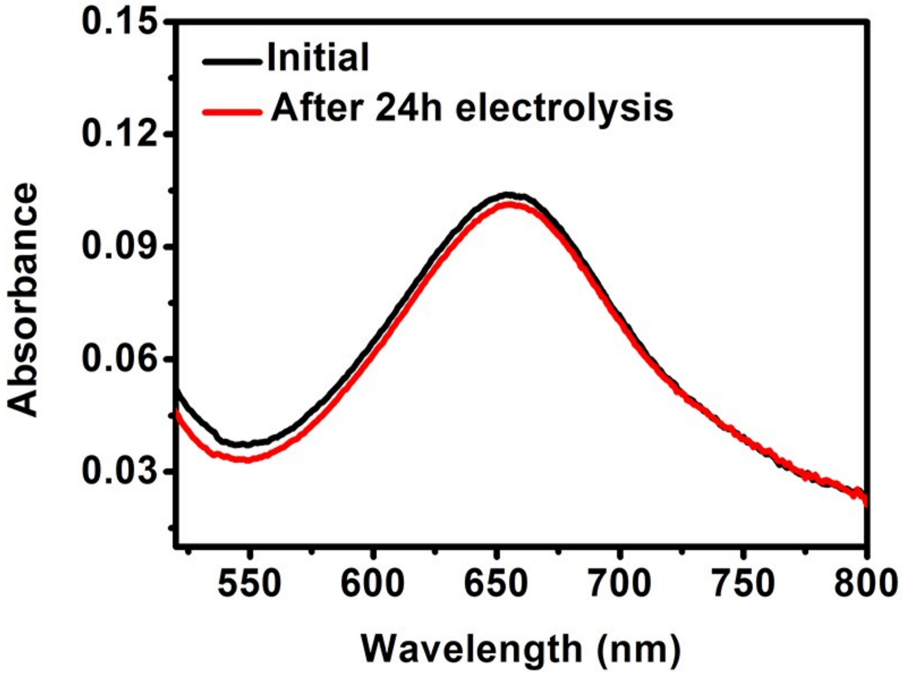

Fig. S14. UV-Vis absorption spectra of the electrolytes stained with indophenol indicator at –0.60 V after electrolysis for 2 h with the initial Bi ND/CP and the Bi ND/CP after 24-h electrolysis.

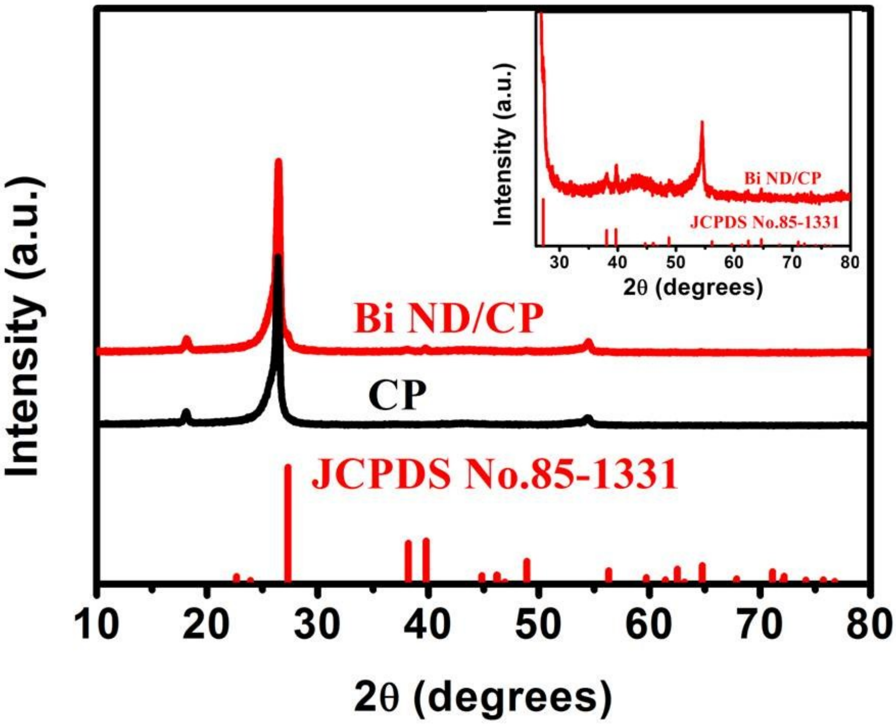

Fig. S15. XRD patterns for Bi ND/CP and CP after stability test.

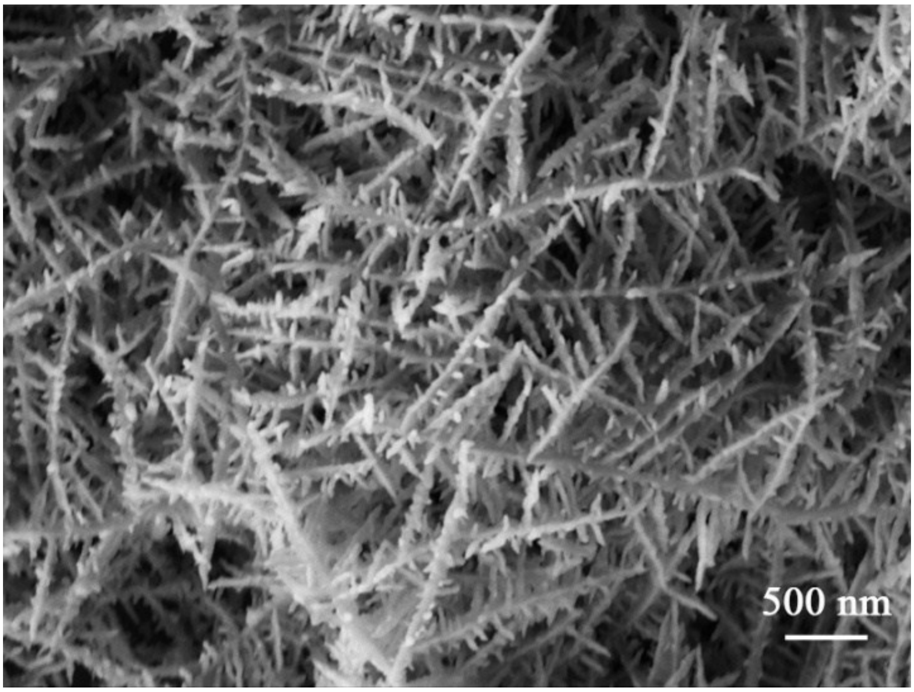

Fig. S16. SEM image for Bi ND after stability test.

Table S1. Comparison of NH_3 yield and FE for Bi ND with reported electrocatalysts under ambient conditions.

Catalyst	Electrolyte	NH_3 yield	FE (%)	Ref.
Bi ND	**0.1 M HCl**	**25.86 μg h^{-1} $mg^{-1}_{cat.}$**	**10.80**	**This work**
N-doped porous carbon	0.1 M HCl	15.7 μg h^{-1} $mg^{-1}_{cat.}$	1.45	4
NPC	0.1 M HCl	0.97 μg h^{-1} $mg^{-1}_{cat.}$	4.2	5
hexagonal BN nanosheet	0.1 M HCl	22.4 μg h^{-1} $mg^{-1}_{cat.}$	4.7	6
Ag nanosheets	0.1 M HCl	2.83 μg h^{-1} $mg^{-1}_{cat.}$	4.8	7
oxygen-doped carbon nanosheet	0.1 M HCl	20.15 μg h^{-1} $mg^{-1}_{cat.}$	4.97	8
TiC/C nanofiber	0.1 M HCl	14.1 μg h^{-1} $mg^{-1}_{cat.}$	5.8	9
Au flowers	0.1 M HCl	25.57 μg h^{-1} $mg^{-1}_{cat.}$	6.05	10
R-WO_3 nanosheet	0.1 M HCl	17.28 μg h^{-1} $mg^{-1}_{cat.}$	7.0	11
$LiMn_2O_4$ NF	0.1 M HCl	15.83 μg h^{-1} $mg^{-1}_{cat.}$	7.44	12
Bi_2MoO_6	0.1 M HCl	20.46 μg h^{-1} $mg^{-1}_{cat.}$	8.17	13
$Ti_3C_2T_x$ nanosheet	0.1 M HCl	20.4 μg h^{-1} $mg^{-1}_{cat.}$	9.3	14
α-Au/CeO_x-RGO	0.1 M HCl	8.31 μg h^{-1} $mg^{-1}_{cat.}$	10.10	15
$Bi_4V_2O_{11}/CeO_2$	0.1 M HCl	23.21 μg h^{-1} $mg^{-1}_{cat.}$	10.16	16
mosaic Bi nanosheet	0.1 M Na_2SO_4	~13.23 μg h^{-1} $mg^{-1}_{cat.}$	10.46±1.45	17
defect-Bi nanoplate	0.2 M Na_2SO_4	5.453 μg h^{-1} $mg^{-1}_{cat.}$	11.6	18
Bi nanosheet array	0.1 M HCl	5.26 μg h^{-1} $mg^{-1}_{cat.}$	10.26	19

References

1 D. Zhu, L. Zhang, R. E. Ruther and R. J. Hamers, *Nat. Mater.*, 2013, **12**, 836–841.

2 G. W. Watt and J. D. Chrisp, *Anal. Chem.*, 1952, **24**, 2006–2008.

3 L. Li, C. Tang, D. Yao, Y. Zheng and S. Qiao, *ACS Energy Lett.*, 2019, **4**, 2111–2116.

4 X. Yang, K. Li, D. Cheng, W. Pang, J. Lv, X. Chen, H. Zang, X. Wu, H. Tan, Y. Wang and Y. Li, *J. Mater. Chem. A*, 2018, **6**, 7762–7769.

5 P. Song, H. Wang, L. Kang, B. Ran, H. Song and R. Wang, *Chem. Commun.*, 2019, **55**, 687–690.

6 Y. Zhang, H. Du, Y. Ma, L. Ji, H. Guo, Z. Tian, H. Chen, H. Huang, G. Cui, A. M. Asiri, F. Qu, L. Chen and X. Sun, *Nano Res.*, 2019, **12**, 919–924.

7 H. Huang, L. Xia, X. Shi, A. M. Asiri and X. Sun, *Chem. Commun.*, 2018, **54**, 11427–11430.

8 H. Huang, L. Xia, R. Cao, Z. Niu, H. Chen, Q. Liu, T. Li, X. Shi, A. M. Asiri, and X. Sun, *Chem. Eur. J.*, 2019, **25**, 1914–1917.

9 G. Yu, H. Guo, W. Kong, T. Wang, Y. Luo, X. Shi, A. M. Asiri, T. Li and X. Sun, *J. Mater. Chem. A*, 2019, **7**, 19657–19661.

10 Z. Wang, Y. Li, H. Yu, Y. Yu, H. Xue, X. Li, H. Wang and L. Wang, *ChemSusChem*, 2018, **11**, 3480–3485.

11 W. Kong, R. Zhang, X. Zhang, L. Ji, G. Yu, T. Wang, Y. Luo, X. Shi, Y. Xu, and X. Sun, *Nanoscale*, 2019, **11**, 19274–19277.

12 C. Li, J. Yu, L. Yang, J. Zhao, W. Kong, T. Wang, A. M. Asiri, Q. Li and X. Sun, *Inorg. Chem.*, 2019, **58**, 9597–9601.

13 Z. Xing, W. Kong, T. Wu, H. Xie, T. Wang, Y. Luo, X. Shi, A. M. Asiri, Y. Zhang and X. Sun, *ACS Sustainable Chem. Eng.*, 2019, **7**, 12692–12696.

14 J. Zhao, L. Zhang, X. Xie, X. Li, Y. Yong, Q. Liu, W. Fang, X. Shi, G. Cui and X. Sun, *J. Mater. Chem. A*, 2018, **6**, 24031–24035.

15 S. Li, D. Bao, M. Shi, B. R. Wulan, J. Yan and Q. Jiang, *Adv. Mater.*, 2017, **29**, 1700001.

16 C. Lv, C. Yan, G. Chen, Y. Ding, J. Sun, Y. Zhou and G. Yu, *Angew. Chem., Int. Ed.*, 2018, **57**, 6073–6073.

17 L. Li, C. Tang, B. Xia, H. Jin, Y. Zheng and S. Qiao, *ACS Catal.*, 2019, **9**, 2902–2908.

18 Y. Wang, M. Shi, D. Bao, F. Meng, Q. Zhang, Y. Zhou, K. Liu, Y. Zhang, J. Wang, Z. Chen, D. Liu, Z. Jiang, M. Luo, L. Gu, Q. Zhang, X. Cao, Y. Yao, M. Shao, Y. Zhang, X. Zhang, J. G. Chen, J. Yan and Q. Jiang, *Angew. Chem., Int. Ed.*, 2019, **58**, 9464–9469.

19 R. Zhang, L. Ji, W. Kong, H. Wang, R. Zhao, H. Chen, T. Li, B. Li, Y. Luo and X. Sun, *Chem. Commun.*, 2019, **55**, 5263–526.